

Spin-Triplet Superconductivity Mediated by Phonons in Quasi-One-Dimensional Systems

Yuuichi SUGINISHI and Hiroshi SHIMAHARA

*Department of Quantum Matter Science, ADSM, Hiroshima University,
Higashi-Hiroshima 739-8530, Japan*

We investigate the spin-triplet superconductivity mediated by phonons in quasi-one-dimensional (Q1D) systems with open Fermi surfaces. We obtain the ground state phase diagrams. It is found that spin-triplet superconductivity occurs for weak screening and strong on-site Coulomb interaction, even in the absence of any additional nonphonon pairing interactions. We find that the nodeless spin-triplet state is more favorable than the spin-triplet state with line nodes, for the parameter values of the Q1D superconductors (TMTSF)₂X. We also find that Q1D open Fermi surface, which is the specific feature of this system, plays an essential role in the pairing symmetry. We discuss the compatibility of the present results with the experimental results in these compounds.

KEYWORDS: anisotropic superconductivity, spin-triplet pairing, phonon-mediated pairing interactions, quasi-one-dimensional systems, organic superconductors, (TMTSF)₂X

1. Introduction

The relation between the symmetry of the superconducting order parameter and the mechanism of the pairing interaction in exotic superconductors is one of the most important subjects in condensed matter physics. In this paper, we are interested in this subject in quasi-one-dimensional (Q1D) systems, in connection with the organic superconductors (TMTSF)₂X with X = PF₆, ClO₄, ...

The compound (TMTSF)₂PF₆ exhibits superconductivity in the proximity of spin-density-wave (SDW) in the phase diagram.¹ Hence, at an early stage after the discovery, the possibility of the superconductivity induced by antiferromagnetic spin fluctuations was proposed.² Takigawa *et al.* have measured the NMR relaxation rate T_1^{-1} in superconducting (TMTSF)₂ClO₄.³ Their results suggest the anisotropic superconducting order parameter with line nodes on the Fermi surface as Hasegawa and Fukuyama argued.⁴ These experimental and theoretical results on T_1^{-1} seem to be consistent with the mechanism of the superconductivity induced by the antiferromagnetic spin fluctuations. In this mechanism, the phase diagram of SDW and *d*-wave superconductivity, whose order parameter has line nodes, has been reproduced semiquantitatively.^{5,6}

However, recent experimental results seem contradictory to one another with respect to the symmetry of the order parameter. Belin and Behnia obtained a temperature dependence of the thermal conductivity in (TMTSF)₂ClO₄ that indicated a nodeless superconducting order parameter.⁷ Their result seems inconsistent with the NMR result mentioned above,³ which indicates the line nodes. As a possible consistent explanation of these results of the NMR and the thermal conductivity, a nodeless *d*-wave superconductivity mediated by antiferromagnetic spin fluctuations has been proposed.⁸ Furthermore, in (TMTSF)₂PF₆ at $P \simeq 6$ kbar and (TMTSF)₂ClO₄, the upper critical field $H_{c2}(T)$ seems

to exceed the Pauli paramagnetic limit H_P at low temperature.^{9,10} From this result of H_{c2} , several authors have discussed possibilities of spin-triplet superconductivity.^{11,12} However, there has not been any observation of a reentrant superconducting phase, which should occur in spin-triplet superconductors at higher field.^{13,14} The experimental result $H_{c2} > H_P$ can be explained by the Fulde-Ferrell-Larkin-Ovchinnikov (FFLO or LOFF) state^{11,15,16} and strong coupling effects. Recently, Lee *et al.* have measured a Knight shift in (TMTSF)₂PF₆ at $P \simeq 0.65$ GPa, the absence of which strongly suggests spin-triplet pairing.¹⁷

Here, we shall briefly summarize the experimental results and pairing symmetries. The full-gap state without any alternation of the sign, which we call *s*-wave state, is consistent with the thermal conductivity, but could not explain the absence of the Hebel-Slichter peak of T_1^{-1} at all,³ as well as the power law behavior and the Knight shift.¹⁷ It is also difficult to explain the phase diagram. Therefore, the *s*-wave state is most unlikely, at least at the present. The singlet state with four line nodes, which we call the *d*-wave state, appeared the most likely at an early stage from the phase diagram and the NMR results, but it could not explain the recent Knight shift results, unless any high-field triplet state is assumed. The thermal conductivity may be explained even in the *d*-wave state with anion order.⁸ The spin-triplet states are compatible with the absence of the Knight shift. For the open Fermi surface, both the full gap spin-triplet state without any line node and that with two line nodes at $k_y = 0$ are possible. We call the former and latter states the *p_x*-wave and *p_y*-wave states, respectively. However, the data of the NMR T_1^{-1} and the thermal conductivity are difficult to be explained consistently. The *p_x*-wave state could explain the thermal conductivity, but could not explain the temperature dependence of $T_1^{-1} \propto T^3$ for $T_c/2 \lesssim T \lesssim T_c$. The coherence peak becomes smaller than that of the *s*-wave state,⁴ but there has not been

any satisfactory theoretical fitting at the present. The p_y -wave state could explain the line node, but it is difficult to reproduce the thermal conductivity. In the p_x and p_y -wave states, the pressure dependence of T_c does not appear to be easily explained as in the d -wave state. Therefore, there is not any perfect explanation consistent for all experimental results at the present.

Many theoretical studies have also been presented in order to clarify the mechanism of superconductivity in these compounds. In Q1D Hubbard models, consistently with early result in the random phase approximation (RPA),⁵ the fluctuation exchange (FLEX) approximation by Kino and Kontani¹⁸ and the third order perturbation theory by Nomura and Yamada¹⁹ have showed that d -wave superconductivity is favorable. Spin-triplet f -wave-like pairing was also examined by Kuroki *et al.*²⁰ There might be a consistent explanation on the basis of f -wave pairing, although f -wave pairing interactions are usually weak, because the f -wave states oscillate many times in the momentum space. Recently, Kohmoto and Sato have discussed the possibility of nodeless spin-triplet superconductivity in a Q1D system with electron-phonon interactions and antiferromagnetic spin fluctuations.²¹

The anisotropic pairing does not necessarily mean the nonphonon mechanism of the pairing interactions. Anisotropic pairing interactions mediated by phonons have been proposed by several authors. Foulkes and Gyroffy argued that p -wave pairing is favorable in metals such as Rh, W and Pd, if the short range Coulomb interaction suppresses the s -wave pairing.²² In connection with high- T_c cuprates, Abrikosov obtained an anisotropic s -wave order parameter in a model of the phonon-mediated interaction with weak Coulomb screening.^{23,24} Moreover, Friedel and Kohmoto, and Chang *et al.* have shown that d -wave superconductivity is induced in a similar model with additional interactions mediated by antiferromagnetic spin fluctuations.^{25,26} More recently, one of the authors and Kohmoto proposed that anisotropic superconductivity can be induced by the phonon-mediated interaction between electrons in ferromagnetic compounds, in connection with UGe₂.²⁷ They also found that the anisotropic pairing interactions are enhanced in layered compounds with a large layer spacing.²⁸ In their paper, they discussed that spin-triplet superconductivity in the compound Sr₂RuO₄ and the organic superconductors may be induced by the phonon-mediated interaction.

In the compound (TMTSF)₂ClO₄, very large isotope shift of T_c was observed,²⁹ which suggests the large contribution of the phonon-mediated interaction to the superconductivity. The large isotope shift may be explained by considering the spin fluctuations.³⁰

In this paper, we investigate the pairing symmetry of Q1D systems within the phonon-mediated pairing interactions. Recently, one of the authors have derived effective Hamiltonians of anisotropic superconductors from a model of electron-phonon systems with coexisting short-range and long-range Coulomb interactions.³¹ We apply these models to the Q1D system. In particular, we examine the phonon-mediated pairing interactions with

screened electron-phonon interactions. Since we are motivated by the above controversy in the Q1D organic compounds (TMTSF)₂X, we are particularly interested in which pairing symmetry is favored in the phonon mechanism for the parameter values of these compounds. However, the range of our study is not limited to these compounds. We are mainly interested in the effects of the open Fermi surface, which is one of the specific features of the Q1D systems. We show that nodeless spin-triplet state (p_x -wave state) is more favorable than the p_y -wave state and the d -wave state in the phonon mechanism.

This paper is constructed as follows: In the next section we introduce the formulation and examine the anisotropic superconductivity mediated by phonons in Q1D systems. In Section 3, we show the results of the numerical calculation and ground state phase diagrams. The last section devoted to the summary and brief discussion.

2. Formalism

2.1 Effective pairing interactions

First, we consider a conventional form of pairing interactions mediated by phonons

$$V_{\text{eff}}(\mathbf{q}, \omega + i\delta) = -g_0 \frac{q_s^2}{|\mathbf{q}|^2 + q_s^2} \frac{[\omega(\mathbf{q})]^2}{\omega^2 - [\omega(\mathbf{q})]^2}, \quad (1)$$

where q_s^{-1} and $\omega(\mathbf{q})$ denote the range of the pairing interaction and the renormalized phonon dispersion energy, respectively. We do not consider the detail of the mechanism of the electron-ion interaction, but only assume the range of the pairing interaction q_s^{-1} . In this sense, our model is phenomenological. This simplification is justified when we are interested in a behavior of the pairing interaction in a length scale larger than the lattice constant. We are mainly interested in the specific feature of the Q1D open Fermi surface. For this purpose, the present model is sufficient. As is referred in ref. 32, near the Fermi surface where $|\omega| < \omega(\mathbf{q})$, the interaction becomes attractive due to the overscreening effect. Except this, we ignore the dynamical effects in this paper. Within the weak coupling theory, the frequency dependence of the pairing interaction $V_{\text{eff}}(\mathbf{q}, \omega + i\delta)$ is simplified as

$$V_{\text{eff}}(\mathbf{q}) = -g \frac{q_s^2}{|\mathbf{q}|^2 + q_s^2}, \quad (2)$$

for $|\xi_{\mathbf{k}}|, |\xi_{\mathbf{k}'}| < \omega_D$, and $V_{\text{eff}}(\mathbf{q}) = 0$ otherwise, where $\mathbf{q} = \mathbf{k} - \mathbf{k}'$, with the Debye frequency ω_D and the electron energy $\xi_{\mathbf{k}}$ measured from the Fermi energy. We assume Q1D band structure with the dispersion relation

$$\xi_{\mathbf{k}} = -2t_a \cos(k_x a_s) - 2t_b \cos(k_y b_s) - \mu \quad (3)$$

where μ , a_s and b_s denote the chemical potential, the intermolecular distances along the a and b directions, respectively. In eq. (2), we have introduced the effective coupling constant g , which depends on the phonon dispersion. Since it is difficult to estimate g_0 and g from the first principle, we regard g as a parameter in this paper. Equation (2) has been studied by many authors.²³⁻²⁸

In the application of eq. (2) to the lattice system, it is more precise to replace $|\mathbf{q}|$ with $\min_{\mathbf{K}} |\mathbf{q} - \mathbf{K}|$.³¹ The

effective interaction of eq. (2) has the peak around $\mathbf{q} = 0$. Actually, the same structures should exist near $\mathbf{q} = \mathbf{K}$, where \mathbf{K} denotes the reciprocal lattice vector. Hence, we obtain the effective Hamiltonian

$$V_{\text{eff}}(\mathbf{q}) = -g \max_{\mathbf{K}} \frac{q_s^2}{|\mathbf{q} - \mathbf{K}|^2 + q_s^2}. \quad (4)$$

We refer to this Hamiltonian as model (a) in this paper.

Secondly, we introduce a model to examine the effect of the corrections due to the charge fluctuations. Within the RPA,^{27,31} the effective interaction is written as

$$V_{\text{eff}}(\mathbf{q}) = -g \max_{\mathbf{K}} \frac{q_s^2}{|\mathbf{q} - \mathbf{K}|^2 + q_s^2 \chi_0(\mathbf{q})/N(0)}. \quad (5)$$

We refer to the Hamiltonian of eq. (5) as model (b). Here, $\chi_0(\mathbf{q})$ denotes the static free susceptibility

$$\chi_0(\mathbf{q}) = \frac{1}{N} \sum_{\mathbf{k}} \frac{f(\xi_{\mathbf{k}}) - f(\xi_{\mathbf{k}+\mathbf{q}})}{\xi_{\mathbf{k}+\mathbf{q}} - \xi_{\mathbf{k}}}, \quad (6)$$

where $f(x) = 1/(e^{x/k_B T} + 1)$. In the original form of this model, we must set $q_s = q_{\text{TF}}$. However, we extend the model by replacing q_{TF}^{-1} with a correct screening length q_s^{-1} so that it includes model (a) with $q_s \neq q_{\text{TF}}$ as a limiting case $\chi_0(\mathbf{q})/N(0) \approx 1$. This replacement of q_{TF} by q_s corresponds to taking into account the vertex correction $\Gamma(\mathbf{k}, \mathbf{k}', \mathbf{q})$ of $v_{\mathbf{q}}$ by an average quantity $\bar{\Gamma}$ with $q_s^2 = \bar{\Gamma} q_{\text{TF}}^2$.

Thirdly, we introduce a model which includes the corrections due to the short-range Coulomb interaction U other than the direct repulsion. Since the details of the derivation are presented in the previous paper,³¹ we shall describe only the outline here. We recall that the pairing interaction mediated by phonons should be proportional to $M_{\mathbf{q}}^2/\kappa_v(\mathbf{q})$ in the absence of U , where $M_{\mathbf{q}}$ and $\kappa_v(\mathbf{q})$ denote the electron-ion coupling constant and the dielectric function due to the long-range Coulomb interaction $v_{\mathbf{q}}$, respectively. The electron-ion interactions are, more or less, the interactions between charges, irrespectively of their details. Therefore, in the presence of U , it is plausible to replace $M_{\mathbf{q}}$ with $M_{\mathbf{q}}/\kappa_U(\mathbf{q})$, where $\kappa_U(\mathbf{q})$ denotes the dielectric function due to U . Furthermore, the polarization function $\chi_0(\mathbf{q})$ in the dielectric function $\kappa_v(\mathbf{q})$ should be replaced by that with a correction due to U , which we write $\chi_U(\mathbf{q})$. In the RPA with respect to U , we have $\kappa_U(\mathbf{q}) = 1 + U\chi_0(\mathbf{q})$ and

$$\chi_U(\mathbf{q}) \equiv \frac{\chi_0(\mathbf{q})}{1 + U\chi_0(\mathbf{q})} = \frac{\chi_0(\mathbf{q})}{\kappa_U(\mathbf{q})}. \quad (7)$$

Therefore, eq. (5) is modified as

$$V_{\text{eff}}(\mathbf{q}) = -\frac{g}{[\kappa_U(\mathbf{q})]^2} \max_{\mathbf{K}} \frac{q_s^2}{|\mathbf{q} - \mathbf{K}|^2 + q_s^2 \chi_U(\mathbf{q})/N(0)}, \quad (8)$$

which we call model (c) in this paper.

The range of effective interaction q_s^{-1} is on the order of the screening length in eq. (4), because it should reflect the range of the Coulomb interaction between electrons and ions. In fact, if we adopt the Thomas-Fermi approximation, we obtain the effective Hamiltonian of the same form as eq. (4) with $q_s = q_{\text{TF}}$. However, we should be careful when we use the Thomas-Fermi approxima-

tion for quantitative purpose on the screening length. For example, in the (TMTSF)₂X systems, the Thomas-Fermi screening length is estimated as $q_{\text{TF}}^{-1} \simeq 1.05 \text{ \AA}$, since $t_a \approx 0.25 \text{ eV}$ and $V_{\text{cell}} \approx 357.2 \text{ \AA}^3$,^{33,34} where V_{cell} denotes the unit cell volume. Hence, q_{TF}^{-1} becomes much smaller than the intermolecular distance $a_s = 3.649 \text{ \AA}$ in the a direction. However, it is obviously underestimation due to the Thomas-Fermi approximation. In practice, we could not apply the Thomas-Fermi approximation to a phenomena of such a short length scale. In the real materials, the screening charges could not exist so densely within the distance shorter than the intermolecular distance a_s . Therefore, for the physical reason, it is more appropriate to assume $q_s^{-1} \gtrsim a_s$ rather than to put $q_s^{-1} = q_{\text{TF}}^{-1}$ in the application to the (TMTSF)₂X systems.

2.2 Gap equation

The gap equation of superconductivity is expressed as

$$\Delta(\mathbf{k}) = -\frac{1}{N} \sum_{\mathbf{k}'} V(\mathbf{k} - \mathbf{k}') \frac{\tanh[E_{\mathbf{k}'}/2k_B T]}{2E_{\mathbf{k}'}} \Delta(\mathbf{k}'), \quad (9)$$

where we have defined $E_{\mathbf{k}'} \equiv \sqrt{\xi_{\mathbf{k}'}^2 + |\Delta(\mathbf{k}')|^2}$, and N denotes the number of the lattice sites. In this gap equation (9), the summation over \mathbf{k}' in the right-hand side is restricted to $|\xi_{\mathbf{k}'}| < \omega_D$ near the Fermi surface. In the numerical calculations, we neglect the temperature dependence on $\chi_0(\mathbf{q})$ since $T \ll t_a$. Further, in the application to the Q1D systems, we put $q_z = 0$ in the effective interaction for simplicity, where the interaction becomes largest. Therefore, we consider only intra-layer pairing in this paper.

Now, we consider the quasi-one-dimensional (Q1D) systems. Once we have obtained the gap equation, the inter-plane electron hopping energy t_c is negligible, while it justifies the BCS mean field approximation for sufficiently low temperature. Near the Fermi surface, we put $\mathbf{k} \simeq (\pm k_{\text{Fx}}(k_y), k_y)$, where the signs $+$ and $-$ correspond to the areas of the Fermi surface of $k_x > 0$ and $k_x < 0$, respectively. Here, $k_{\text{Fx}}(k_y)$ is the Fermi wave vector of the k_x direction at k_y . Then, we can write

$$\begin{aligned} V(\mathbf{k} - \mathbf{k}') &\simeq V(k_{\text{Fx}}(k_y) \mp k_{\text{Fx}}(k'_y), k_y - k'_y) \\ &\equiv \begin{cases} V^{(++)}(k_y, k'_y) = V^{(--)}(k_y, k'_y) \\ V^{(+-)}(k_y, k'_y) = V^{(-+)}(k_y, k'_y) \end{cases} \end{aligned} \quad (10)$$

and $\Delta(\mathbf{k}) \simeq \Delta^{(\text{sign}(k_x))}(k_y)$. In the weak-coupling limit, one readily finds that the gap equation (9) near the superconducting transition temperature T_c takes the form

$$\begin{aligned} \begin{pmatrix} \Delta^{(+)}(k_y) \\ \Delta^{(-)}(k_y) \end{pmatrix} &= -\frac{1}{\lambda} \int_{-\pi/b}^{\pi/b} \frac{b dk'_y}{2\pi} \rho(k'_y) \\ &\begin{pmatrix} V^{(++)}(k_y, k'_y) & V^{(+-)}(k_y, k'_y) \\ V^{(-+)}(k_y, k'_y) & V^{(--)}(k_y, k'_y) \end{pmatrix} \begin{pmatrix} \Delta^{(+)}(k'_y) \\ \Delta^{(-)}(k'_y) \end{pmatrix}, \end{aligned} \quad (11)$$

where we have defined the density of states $\rho(k'_y) =$

$1/4\pi t_a \sin[k_{F_x}(k'_y)a]$ and

$$\frac{1}{\lambda} = \ln \left[\frac{2e^\gamma \omega_D}{\pi k_B T_c} \right] \quad (12)$$

with the Euler constant $\gamma = 0.57721 \dots$.

This matrix equation (11) is easily diagonalized and one obtains

$$\hat{\Delta}^D(k_y) = -\frac{1}{\lambda} \int_{-\pi/b}^{\pi/b} \frac{b dk'_y}{2\pi} \hat{V}^D(k_y, k'_y) \hat{\Delta}^D(k'_y) \quad (13)$$

with

$$\hat{\Delta}^D(k_y) = \sqrt{\rho(k_y)} \begin{pmatrix} \Delta^{(+)}(k_y) + \Delta^{(-)}(k_y) \\ \Delta^{(+)}(k_y) - \Delta^{(-)}(k_y) \end{pmatrix} \equiv \begin{pmatrix} \tilde{\Delta}^s(k_y) \\ \tilde{\Delta}^a(k_y) \end{pmatrix} \quad (14)$$

and

$$\hat{V}^D(k_y, k'_y) \equiv \begin{pmatrix} \tilde{V}^{(++)} + \tilde{V}^{(+-)} & 0 \\ 0 & \tilde{V}^{(++)} - \tilde{V}^{(+-)} \end{pmatrix}, \quad (15)$$

where we have defined

$$\tilde{V}^{(ss')}(k_y, k'_y) \equiv \sqrt{\rho(k_y)} V^{(ss')}(k_y, k'_y) \sqrt{\rho(k'_y)}. \quad (16)$$

We expand the effective interaction and the order parameter on the Fermi surface as

$$\tilde{V}^{(ss')}(k_y, k'_y) = \sum_{m=0}^{\infty} \sum_{n=0}^{\infty} \left[\tilde{V}_{mn}^{(ss')} \gamma_m(k_y) \gamma_n(k'_y) + \tilde{\bar{V}}_{mn}^{(ss')} \bar{\gamma}_m(k_y) \bar{\gamma}_n(k'_y) \right] \quad (17)$$

and

$$\tilde{\Delta}^\alpha(k_y) = \sum_{m=0}^{\infty} \left[\tilde{\Delta}_m^\alpha \gamma_m(k_y) + \tilde{\bar{\Delta}}_m^\alpha \bar{\gamma}_m(k_y) \right] \quad (18)$$

with $\alpha = s$ or a , which correspond to symmetric and antisymmetric states with respect to k_x , respectively. Here, we have defined $\gamma_m(k_y) = n_m \cos(mk_y b)$ and $\bar{\gamma}_m(k_y) = n_m \sin(mk_y b)$, and the normalization factors $n_m = \sqrt{2}$ for $m \neq 0$ and $n_m = 1$ for $m = 0$. The expansion factors are given by

$$\begin{aligned} \tilde{V}_{mn}^{(ss')} &= \int_{-\pi/b}^{\pi/b} \frac{b dk_y}{2\pi} \int_{-\pi/b}^{\pi/b} \frac{b dk'_y}{2\pi} \\ &\quad \times \gamma_m(k_y) \tilde{V}^{(ss')}(k_y, k'_y) \gamma_n(k'_y), \\ \tilde{\bar{V}}_{mn}^{(ss')} &= \int_{-\pi/b}^{\pi/b} \frac{b dk_y}{2\pi} \int_{-\pi/b}^{\pi/b} \frac{b dk'_y}{2\pi} \\ &\quad \times \bar{\gamma}_m(k_y) \tilde{\bar{V}}^{(ss')}(k_y, k'_y) \bar{\gamma}_n(k'_y). \end{aligned} \quad (19)$$

By inserting eqs. (17) and (18) into the gap equation (13), we obtain matrix equations

$$\begin{aligned} \sum_{n=0}^{\infty} \lambda_{mn}^\alpha \Delta_n^\alpha &= \lambda \Delta_m^\alpha, \\ \sum_{n=0}^{\infty} \bar{\lambda}_{mn}^\alpha \bar{\Delta}_n^\alpha &= \lambda \bar{\Delta}_m^\alpha, \end{aligned} \quad (20)$$

Table I. The classification of the possible pairing states and relevant components of the gap functions.

	$\gamma_m(k_y)$	$\bar{\gamma}_m(k_y)$
$\alpha = s$	Δ_0^s : s -wave state Δ_1^s : d -wave state	$\bar{\Delta}_1^s$: p_y -wave state
$\alpha = a$	Δ_0^a : p_x -wave state	$\bar{\Delta}_1^a$: d_{xy} -wave state

where

$$\begin{aligned} \lambda_{mn}^s &= -(V_{mn}^{(++)} + V_{mn}^{(+-)}), \\ \lambda_{mn}^a &= -(V_{mn}^{(++)} - V_{mn}^{(+-)}), \\ \bar{\lambda}_{mn}^s &= -(\bar{V}_{mn}^{(++)} + \bar{V}_{mn}^{(+-)}), \\ \bar{\lambda}_{mn}^a &= -(\bar{V}_{mn}^{(++)} - \bar{V}_{mn}^{(+-)}). \end{aligned} \quad (21)$$

We summarize our notation in Table I.

With the maximum eigenvalue λ , the superconducting transition temperature T_c is given by

$$k_B T_c = \frac{2e^\gamma}{\pi} \omega_D \exp[-1/\lambda], \quad (22)$$

for $\lambda > 0$.

Here, we note that the Coulomb pseudo-potential μ_C^* defined by

$$\mu_C^* = \frac{UN(0)}{1 + UN(0) \ln(W_c/\omega_D)} \quad (23)$$

must be subtracted from the eigenvalue λ for the s -wave state obtained above.²⁸ Here, W_c is the cutoff energy on the order of the bandwidth. It is obvious that the on-site Coulomb repulsive interaction U is not included in models (a)-(c), except the corrections due to U in the electron-phonon interaction and the screening function in model (c). However, it reduces only the s -wave pairing interaction, because of the symmetry. For example, in (TMTSF)₂X, it is estimated to be $U \simeq 1.5t_a$ from the SDW transition temperature at $t_b = 0.1t_a$.⁵

At this point, we have three parameters, the effective electron-phonon coupling constant g , the screening length q_s^{-1} and the on-site Coulomb interaction U . Furthermore, we shall consider the electron number n per a site and a spin, the transfer integral t_b and the ratio a_s/b_s as given parameters within the Q1D systems with open Fermi surfaces. Here, for exchanging particle and hole, it is easily verified that the results for n and for $n-1$ are equivalent to each other. For example, $n = 1/4$ and $n = 3/4$ give the same results below.

3. Results

In this section, we show the results of the numerical calculations. In Figs. 1-9, we set $\omega_D = 200$ K,³⁵ $t_b/t_a = 0.1$ (except for Fig. 6), $n = 1/4$ (except for Fig. 5) and $a_s/b_s = 0.468$ (except for Figs. 2 and 7), considering the compounds (TMTSF)₂X. These compounds have a slight strain of the lattice, but we have confirmed by the numerical calculations that it changes the result only very slightly. Therefore, we only show the results when the crystal axes are orthogonal. We set $W_c/\omega_D = 25.12$ in μ_C^* from the experimental values,³⁵

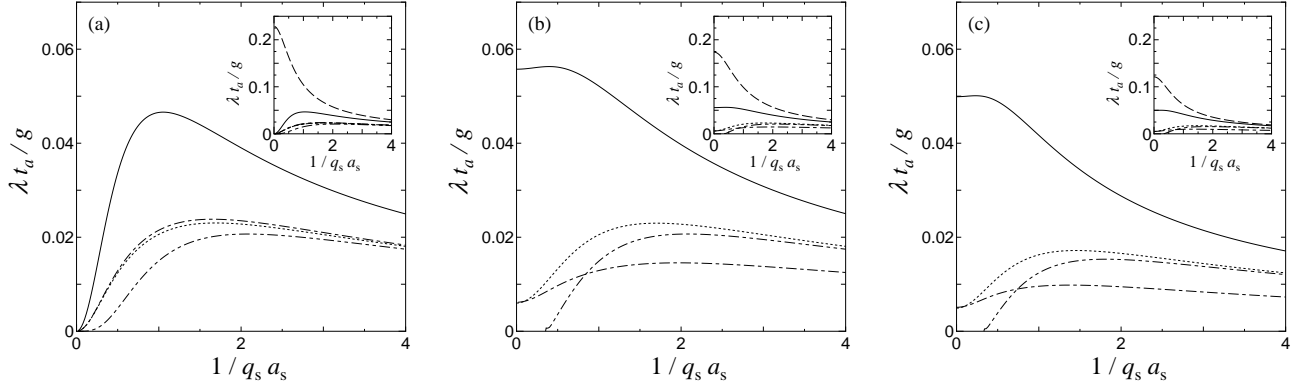


Fig. 1. The dimensionless coupling constants λ as functions of the screening length q_s^{-1} . The labels (a), (b) and (c) correspond to the names of the models. The solid, dotted, dot-dashed and 2-dot-dashed curves show the coupling constants λ for p_x , p_y , d and d_{xy} -wave pairing, respectively. In the inset, the dashed curve shows the result for the s -wave state.

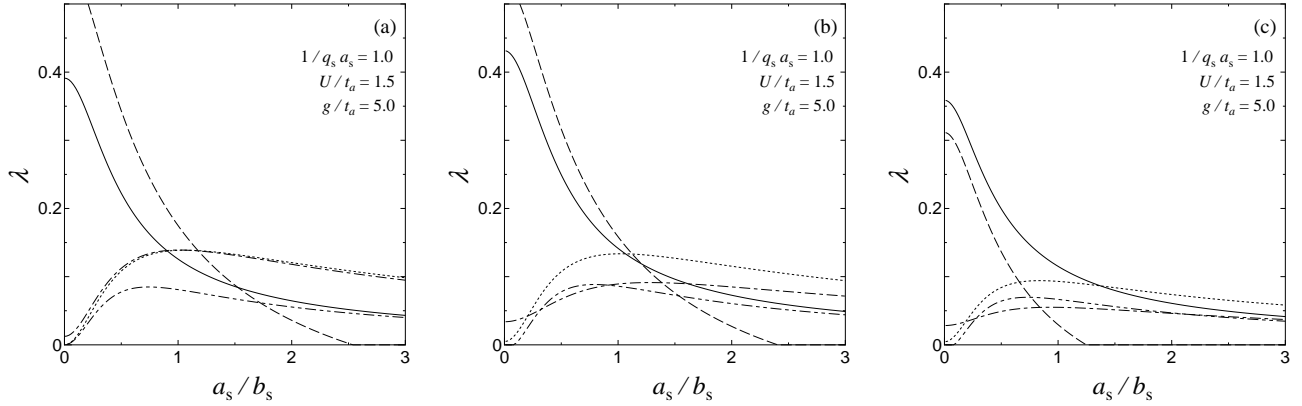


Fig. 2. The dimensionless coupling constants λ as functions of the ratio a_s/b_s . The labels (a), (b) and (c) correspond to the names of the models. The solid, dotted, dashed, dot-dashed and 2-dot-dashed curves represent the results of λ for p_x , p_y , s , d and d_{xy} -wave pairing, respectively. The Coulomb parameter μ_C^* is subtracted from λ of s -wave pairing.

since $W_c = \sqrt{(W - \mu')\mu'} \approx \sqrt{3}t_a^{31}$ for 1/4-filled band, where W and μ' denote the band width and the chemical potential measured from the bottom of the band, respectively.

In Fig. 1, the results of the dimensionless coupling constants λ are shown as functions of the screening length q_s^{-1} . The labels (a)-(c) of figures correspond to the name of the models, which have been defined in the previous section. The s -wave coupling constant decreases rapidly with increase of the screening length $(q_s a_s)^{-1}$ and is close to anisotropic coupling constants in $(q_s a_s)^{-1} \gtrsim 1.0$. In a whole region of $(q_s a_s)^{-1}$, the p_x -wave state is more favorable than the p_y -wave state. Especially for large $(q_s a_s)^{-1}$, the p_x -wave state can easily overcome the s -wave state with an assistance of μ_C^* . We find the similar behavior in models (a)-(c) for $(q_s a_s)^{-1} \gtrsim 1.0$.

Figure 2 shows the dimensionless coupling constants λ as functions of the ratio a_s/b_s . We assume $(q_s a_s)^{-1} = 1.0$, $U/t_a = 1.5$ and $g/t_a = 5.0$ as an example. The p_y -wave state is favored for $a_s/b_s \gtrsim 1.0$, while p_x -wave state is favored for $a_s/b_s \lesssim 1.0$, when s -wave state is suppressed. In Figs. 1 and 2, it is also found by comparison the results of models (a)-(c) that the s -wave pairing interaction is weakened by the corrections due to the charge fluctuation

and the short-range Coulomb interaction apart from μ_C^*

In Figs. 3-9, we concentrate ourselves to model (c). The results are qualitatively the same as those in models (a) and (b).

Figure 3 shows the phase diagram at $T = 0$ in the $(q_s a_s)^{-1} - U/t_a$ plane. The parameter $g/t_a = 5.0$ is taken as an example. It is found that the p_x -wave superconductivity occurs in the region where the screening effect is weak and the short-range interaction U is strong.

Figure 4 shows the phase diagrams at $T = 0$ in the $g/t_a - U/t_a$ plane. In each phase diagram, as is printed in it, the parameter $(q_s a_s)^{-1} = 0.3, 1.0$ are taken as examples. It is found that the p_x -wave superconductivity is favored for weak electron-phonon coupling and weak Coulomb screening.

Figure 5 shows the phase diagram at $T = 0$ in the $n - U/t_a$ plane. We show the results in the region of n where the Fermi surface is open. We set $(q_s a_s)^{-1} = 1.0$ and $g/t_a = 5.0$ as an example. The p_x -wave superconductivity is favored for large n .

Figure 6 shows the phase diagram at $T = 0$ in the $t_b/t_a - U/t_a$ plane. We set $(q_s a_s)^{-1} = 1.0$ and $g/t_a = 5.0$ as an example. It is found that when t_b/t_a increases, the p_x -wave superconductivity is suppressed. Figure 7 shows

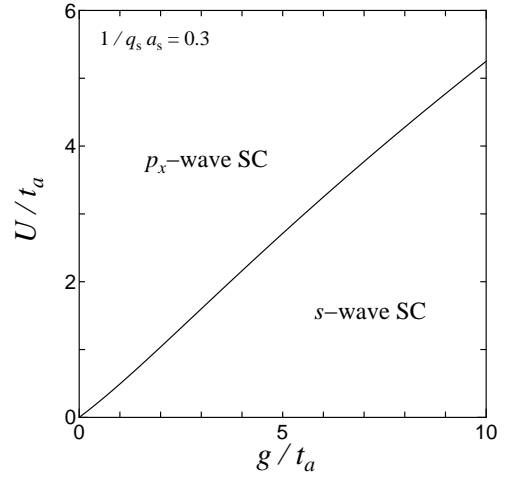
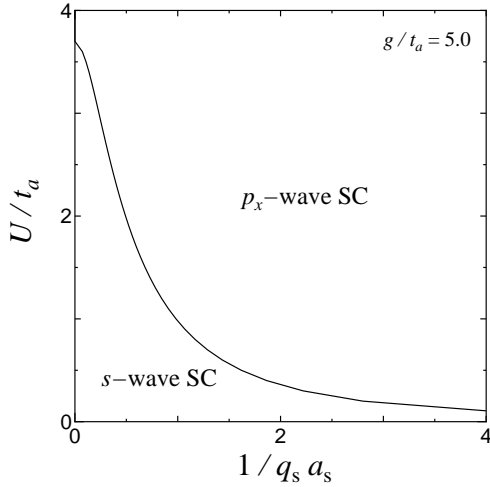


Fig. 3. The $q_s^{-1}U$ phase diagram at $T = 0$ in model (c). Here, SC stands for superconductivity.

the phase diagrams at $T = 0$ in the $a_s/b_s - U/t_a$ plane. The parameters, $g/t_a = 5.0$, $(q_s a_s)^{-1} = 0.3$ or 1.0 are taken as examples. It is found that the p_x -wave state is favored for small a_s , while the p_y -wave state is favored for large a_s .

These results are physically interpreted as follows. The phonon-mediated pairing interactions are attractive in a whole momentum space of $\mathbf{q} = \mathbf{k} - \mathbf{k}'$, and have a peak at $\mathbf{q} = 0$. Thus, the order parameter $\Delta(\mathbf{k})$ at \mathbf{k} is favorable if $\Delta(\mathbf{k}')$'s of $\mathbf{k}' \approx \mathbf{k}$ have the same sign as $\Delta(\mathbf{k})$, while unfavorable if $\Delta(\mathbf{k}')$'s at $\mathbf{k}' \approx \mathbf{k}$ have the opposite sign as $\Delta(\mathbf{k})$. Therefore, the p_y -wave state is originally more unfavorable than the p_x -wave state, because of the node at $k_y = 0$, where $\Delta(\mathbf{k})$ changes its sign. However, when the areas of the Fermi surfaces of $k_x > 0$ and $k_x < 0$ approach by increasing a_s , the p_x -wave state becomes unfavorable, because $\Delta(k_x > 0, k_y)$ and $\Delta(k_x < 0, k_y)$ have opposite signs. The dependences on t_b of the coupling constants are also explained in the same manner as the dependences on the ratio a_s/b_s . Near the ends of the first Brillouin zone, the distance between the sheets of the Fermi surface becomes narrower as t_b increase. (For $t_b/t_a \gtrsim 0.35$, the Fermi surface is closed.) For the p_x -wave state, the interaction becomes repulsive for pair hopping $\Delta(\mathbf{k}) \rightarrow \Delta(\mathbf{k}')$ near the zone ends. As a result, as t_b increases, s -wave superconductivity becomes more favorable than p_x -wave one.

Figures 8 and 9 show the calculated momentum dependences of the order parameters. We assume $(q_s a_s)^{-1} = 1.0$ and $U/t_a = 1.5$ as an example in both figures. It is confirmed that the p_y and d_{xy} -wave states have a line node on the Fermi surface at $k_y = 0$, the d -wave state has line nodes at $k_y \approx \pm\pi/2b$, and the s and p_x -wave states are full gap states.

4. Summary and Discussion

Now, we summarize the results. We have examined pairing interactions mediated by phonons in quasi-one-dimensional (Q1D) systems with open Fermi surfaces. It was found that spin-triplet superconductivity occurs

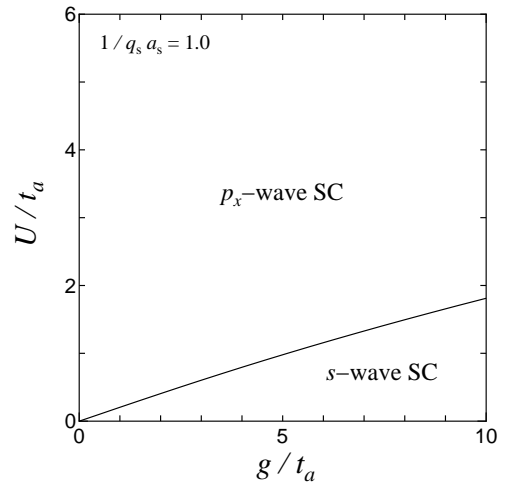
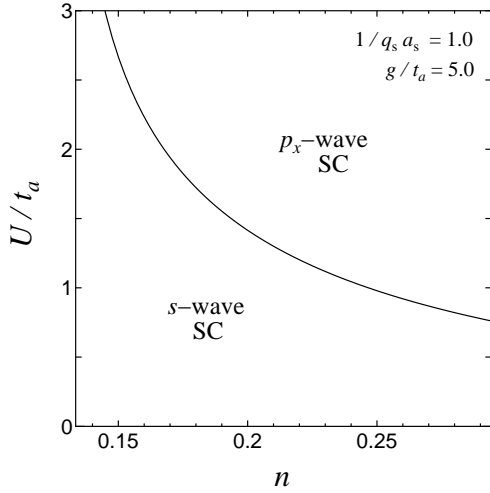
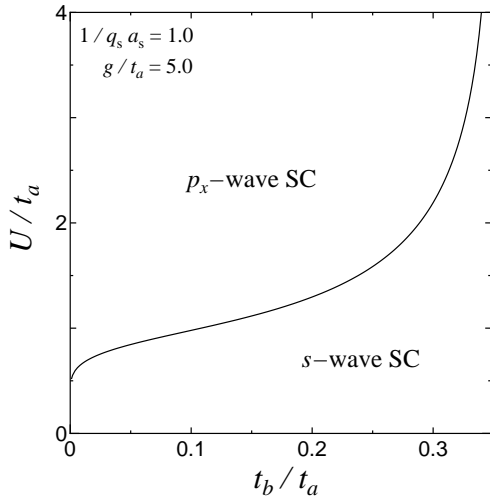


Fig. 4. The phase g - U diagrams at $T = 0$ in model (c).

for weak Coulomb screening and strong on-site Coulomb interaction U , even in the absence of any additional non-phonon pairing interactions. We have examined two possible spin-triplet states. One has a nodeless gap function $\Delta(\mathbf{k})$ for the open Fermi surface, while another has line nodes at $k_y = 0$ on the Fermi surface. We call the former p_x -wave state, while the latter p_y -wave state. We have found that when the Fermi surface is open, the larger the ratio a_s/b_s is, the more favorable p_y -wave superconductivity becomes. We have explained the physical reason for it. It was argued that the p_x -wave state occurs when the conductive chains are separated with a sufficiently large spacing.

In $(\text{TMTSF})_2\text{X}$, the ratio $a_s/b_s = 0.468$ and the hole density $n = 1/4$ give sufficiently large separation of the $k_x > 0$ and $k_x < 0$ sheets of the open Fermi surface when $t_b = 0.1t_a$. Hence, the p_x -wave state is more favorable than the p_y -wave state in those compounds. It was also found that the p_x -wave state is more favorable than the s -wave state for $n = 1/4$ and $U \approx 1.5t_a$, which are appropriate to $(\text{TMTSF})_2\text{X}$, if we set $(q_s a_s)^{-1} \gtrsim 1.0$, which is physically plausible.

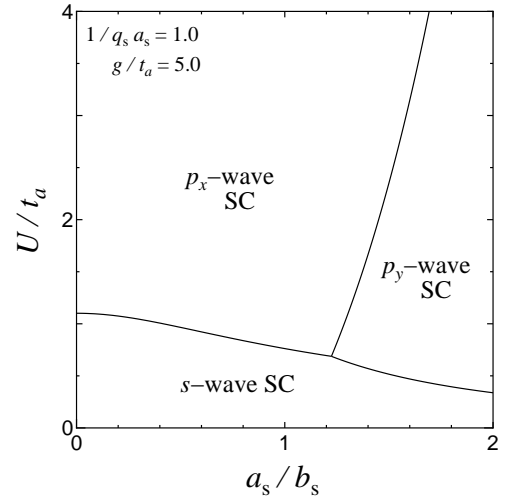
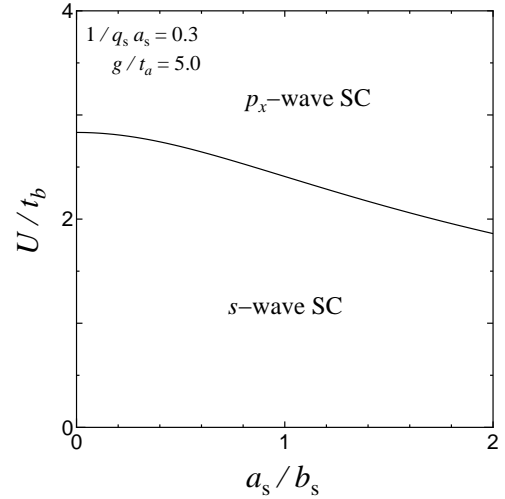
In our model, t_b may be regarded as an effective parameter that reflects an effect of pressure. If a_s/b_s and t_b

Fig. 5. The n - U phase diagram at $T = 0$ in model (c).Fig. 6. The t_b - U phase diagram at $T = 0$ in model (c).

increase with increase of the pressure, the coupling constant for p_x -wave pairing decreases as found in Figs. 2 and 6. This pressure dependence may contribute to the observed pressure dependence of T_c to some extent.

In order to discuss the reality of the phonon-mediated spin-triplet superconductivity, we crudely estimate the parameters for $(\text{TMTSF})_2\text{X}$ from the observed transition temperature $T_c \simeq 1.0$ K. Here, we assume p_x -wave pairing. If we assume $\omega_D \simeq 200$ K³⁵ and $T_c \simeq 1.0$ K, we have $\lambda \simeq 0.184$. Then we find $g \simeq 4.61t_a$ for $(q_s a_s)^{-1} \simeq 1.0$ from Fig. 1. For such a choice of parameter values, in order to suppress s -wave pairing, the on-site Coulomb repulsion must be $U \gtrsim 2t_a \simeq 0.5W$, which seems realistic as the order of the magnitude. This value is rather larger than the estimation $U \approx 1.5t_a$ from the SDW transition. However, it can be explained that in practice, the repulsive on-site interaction is enhanced by the spin fluctuation near the SDW phase from the bare value U .

In conclusion, in the compounds $(\text{TMTSF})_2\text{X}$, the nodeless spin-triplet superconductivity is favorable if s -wave superconductivity is suppressed. The present result

Fig. 7. The a_s/b_s - U phase diagrams at $T = 0$ in model (c).

consistent with the experimental data of the Knight shift and thermal conductivity. Moreover, it was also found that the following three conditions are indispensable for the appearance of the nodeless spin-triplet superconductivity: (1) The screening effect is sufficiently weak; (2) The short-range Coulomb interaction is strong; (3) The distance between sheets of the open Fermi surface is sufficiently large. Here, conditions (1) and (2) are satisfied in $(\text{TMTSF})_2\text{X}$, in which it is known that the electron states are well-described by the tight-binding model, and the layer spacing is large. The condition (3) is satisfied by the quasi-one-dimensionality ($a_s/b_s = 0.468$) and the hole density $n = 1/4$.

In $(\text{TMTSF})_2\text{X}$, the pressure-temperature phase diagrams of superconductivity and SDW were obtained.¹ The pressure dependence may be reproduced by taking into account the pairing interactions mediated by anti-ferromagnetic fluctuations, since those interactions have attractive triplet components.^{5,36} We have also shown that the p_x -wave interaction decreases to some extent as the pressure increases. The explanation of the experimental phase diagrams in the present theory including the effect of the spin fluctuations remains for a future

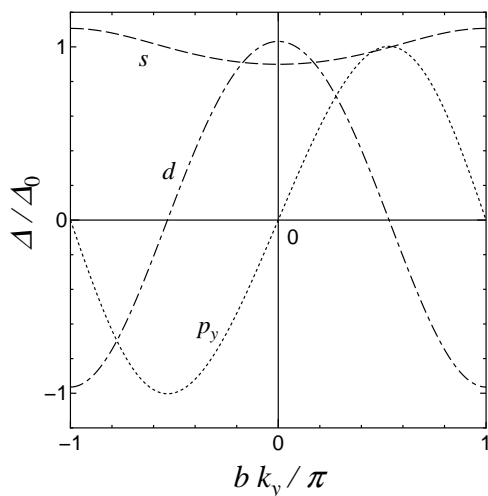


Fig. 8. The momentum dependences of the order parameters $\Delta(k_{Fx}(k_y), k_y)$ of s , p_y and d -wave states in model (c). In these states, $\Delta(k_x, k_y) = \Delta(-k_x, k_y)$.

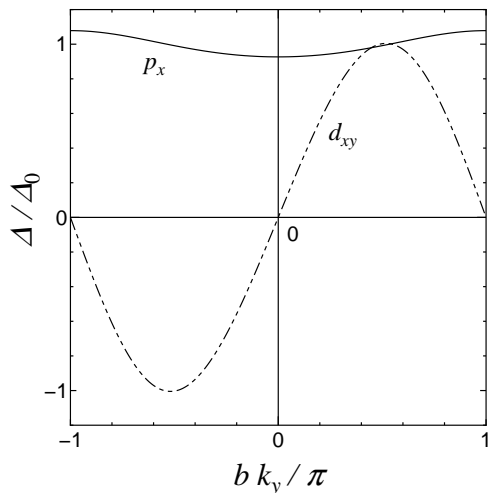


Fig. 9. The momentum dependences of the order parameters $\Delta(k_{Fx}(k_y), k_y)$ of p_x and d_{xy} -wave states in model (c). In these states, $\Delta(k_x, k_y) = -\Delta(-k_x, k_y)$.

study.

Acknowledgment

This work was partly supported by a Grant-in-Aid for COE Research (No.13CE2002) of the Ministry of Education, Culture, Sports, Science and Technology of Japan.

- 1) D. Jérôme: *Mol. Cryst. Liq. Cryst.* **79** (1982) 155.
- 2) V.J. Emery: *Synth. Met.* **13** (1986) 21.

- 3) M. Takigawa, H. Yasuoka and G. Saito: *J. Phys. Soc. Jpn.* **56** (1987) 873.
- 4) Y. Hasegawa and H. Fukuyama: *J. Phys. Soc. Jpn.* **56** (1987) 877.
- 5) H. Shimahara: *J. Phys. Soc. Jpn.* **58** (1989) 1735.
- 6) In p. 272 of ref. 33, it is claimed that since $T_{SDW} = 25$ K is assumed at $t_b = 0$ in ref. 5, the obtained $T_c \lesssim 1.0$ K is slightly too low. However, in actuality, $T_{SDW} = 20$ K is assumed at $t_b = 0$ in ref. 5, and it gives $T_{SDW} \simeq 12$ K at $t_b = 0.1t_a$, which agrees with the experimental facts.
- 7) S. Belin and K. Behnia: *Phys. Rev. Lett.* **79** (1997) 2125.
- 8) H. Shimahara: *Phys. Rev. B* **61** (2000) 14936(R).
- 9) I.J. Lee, M.J. Naughton, G.M. Danner and P.M. Chaikin: *Phys. Rev. Lett.* **78** (1997) 3555.
- 10) J.I. Oh and M.J. Naughton: *Phys. Rev. Lett.* **92** (2004) 067001.
- 11) A.G. Lebed, K. Machida and M. Ozaki: *Phys. Rev. B* **62** (2000) 795(R).
- 12) C.D. Vaccarella and C.A.R. Sá de Melo: *Phys. Rev. B* **64** (2001) 212504.
- 13) A.G. Lebed: *Pis'ma Zh. Eksp. Teor. Fiz.* **44** (1986) 89 [JETP Lett. **44** (1986) 114].
- 14) N. Dupuis, G. Montanboux and C.A.R. Sá de Melo: *Phys. Rev. Lett.* **70** (1993) 2613.
- 15) M. Miyazaki and Y. Hasegawa: *J. Phys. Soc. Jpn.* **65** (1996) 3283.
- 16) H. Shimahara: *Phys. Rev. B* **62** (2000) 3524.
- 17) I.J. Lee, S.E. Brown, W.G. Clark, M.J. Strouse, M.J. Naughton, W. Kang and P.M. Chaikin: *Phys. Rev. Lett.* **88** (2002) 017004.
- 18) H. Kino and H. Kontani: *J. Phys. Soc. Jpn.* **68** (1999) 1481.
- 19) T. Nomura and K. Yamada: *J. Phys. Soc. Jpn.* **70** (2001) 2694.
- 20) K. Kuroki, R. Arita and H. Aoki: *Phys. Rev. B* **63** (2001) 094509.
- 21) M. Kohmoto and M. Sato: *Europhys. Lett.* **56** (2001) 736.
- 22) I.F. Foulkes and B.L. Gyorffy: *Phys. Rev. B* **15** (1977) 1395.
- 23) A.A. Abrikosov: *Physica C* **222** (1994) 191.
- 24) A.A. Abrikosov: *Physica C* **224** (1995) 243.
- 25) J. Friedel and M. Kohmoto: *Int. J. Mod. Phys. B* **15** (2001) 511.
- 26) I. Chang, J. Friedel and M. Kohmoto: *Europhys. Lett.* **50** (2000) 782.
- 27) H. Shimahara and M. Kohmoto: *Europhys. Lett.* **57** (2002) 247.
- 28) H. Shimahara and M. Kohmoto: *Phys. Rev. B* **65** (2002) 174502.
- 29) H. Schwenk, E. Hess, K. Andres F. Wudl and E. Aharon-Shalom: *Phys. Lett. A* **102** (1984) 57.
- 30) H. Shimahara: *J. Phys. Soc. Jpn.* **72** (2003) 1851.
- 31) H. Shimahara: cond-mat/0403628 (unpublished).
- 32) J.R. Schrieffer: *Theory of Superconductivity* (revised ed.), (W.A. Benjamin, New York, 1983).
- 33) See, for example, T. Ishiguro, K. Yamaji and G. Saito: *Organic Superconductors* (2nd ed.), (Springer-Verlag, Berlin, 1998).
- 34) In actuality, the unit cell volume of $(\text{TMTSF})_2\text{PF}_6$ is 714.3 \AA^3 .³³ However, since the anions are far from the conduction layers of TMTSF molecules, we regard that the unit cell consists of a single TMTSF molecule. Therefore, in our model, we set $V_{\text{cell}} = 714.3/2 = 357.2 \text{ \AA}^3$.
- 35) The value of the Debye frequency $\omega_D = 198$ K was obtained by the specific heat measurement in H. Yang, J.C. Lasjaunias and P. Monceau: *J. Phys.: Condens. Matter* **11** (1999) 5083.
- 36) H. Shimahara: *J. Phys. Soc. Jpn.* **69** (2000) 1966.